PHYSICAL REVIEW B VOLUME 31, NUMBER 10 15 MAY 1985

# Anisotropy of the high-energy satellites of the $K$ emission band in graphite

A. Mansour, S. E. Schnatterly, and R. D. Carson
*Physics Department, University of Virginia, Charlottesville, Virginia 22901*

(Received 26 November 1984)

Two satellites on the high-energy side of the $K$ emission band of graphite have been observed and found to be anisotropic. One of them is attributed to the radiative decay of double ionization of the $K$ shell while the other is tentatively explained as resulting from electronic transitions from the conduction-band minimum into the $K$-shell vacancy.

## INTRODUCTION

Radiative transitions of valence electrons into core holes give rise to soft x-ray emission bands. Weak features are often observed on the high-energy side of a main band and are referred to as satellites. These satellites were first observed in 1916[1] and have usually been attributed to the radiative decay of multiply ionized atoms. Other origins have been proposed as well, and a number of review articles have been published.[2–4]

In this paper we report the observation of two satellites on the high-energy side of the $K$ emission band of graphite. Neither of these have been seen before in graphite, although one has been seen in the compound $B_4C$,[5] where it was attributed to a double ionization of the carbon $1S$ level. Our sample consists of small graphite particles deposited on a surface. Emission from such a sample is anisotropic, with $\sigma$ and $\pi$ valence electrons contributing differently to the emission spectrum at any given angle.[6–10] We expect the satellites to be anisotropic as well. By varying the take-off angle of the x-ray emission relative to the sample normal, we have been able to separate the satellites into $\sigma$ and $\pi$ components. The shapes of these bands are presented and their origins discussed.

## EXPERIMENTAL APPARATUS

The soft x-ray emission spectrograph used for the measurements has been previously described.[11,12] The samples are excited with an electron beam and the emitted x rays dispersed by a toroidal diffraction grating used at grazing incidence. The detector is a position-sensitive multielement photodiode array. The calibration accuracy in the energy range of interest is approximately 0.2 eV.

Samples were prepared by spraying graphite particles suspended in alcohol onto a substrate where they formed a highly ordered polycrystalline sample. Granular samples were used rather than highly ordered pyrolytic graphite (HOPG) because we found them to be of higher purity. A rotatable sample holder was used which allowed the take-off angle measured from the sample normal to be varied between 0° and 80° without breaking vacuum. The vacuum in the sample chamber was maintained in the low $10^{-9}$-torr range. The excitation electron beam energy was varied between 1.5 and 3 kV while the current was maintained at 1.5 mA.

## THEORETICAL BACKGROUND

In the one-electron model of soft x-ray emission the emission intensity at energy $E=\hbar\omega$ can be expressed as

$$I(\omega)\propto\omega\int d^3k\,F(E,\mathbf{k})\delta(E_v(\mathbf{k})-E_c-\hbar\omega)\Theta(E_F-E_v(\mathbf{k}))\ , \tag{1}$$

where the integration is over a surface $S$ of constant energy in reciprocal space, and $F(E,k)$ is the square of the transition matrix element:

$$F(E,\mathbf{k})=|\langle\tau_{\text{core}}\,|\,\mathbf{p}\cdot\mathbf{A}\,|\,\tau_{\text{valence}}(\mathbf{k})\rangle|^2\ , \tag{2}$$

where $\mathbf{A}$ is the vector potential. In the dipole approximation $F(E,\mathbf{k})$ can be simplified to

$$F(E,\mathbf{k})=A_0^2D^2\cos^2\theta\ , \tag{3}$$

where $D=\langle\tau_c\,|\,\mathbf{x}\,|\,\tau_v\rangle$ is the dipole moment vector and $\theta$ is the angle between $A$ and $D$.

Graphite is a layered material consisting of hexagonal planes of carbon atoms. The strong covalent bonding within a layer is due to $2P_x$, $2P_y$, and $2s$ electrons, referred to as $\sigma$ electrons. The $2P_z$ electrons with wave-function lobes oriented perpendicular to the hexagonal layers are referred to as $\pi$ electrons. The $\pi$ bonds are weaker than the $\sigma$ bonds, and are responsible for the metallic character of graphite.

In the dipole approximation for transitions into a $1s$ core level the $\sigma$ electrons will give rise to an angle-dependent emission pattern corresponding to $x$ and $y$ oriented dipoles oscillating in the hexagonal layer:

$$I_\sigma(E,\theta)=I_\sigma(E)\left[\frac{1+\cos^2\theta}{2}\right]\ ,$$

where $\theta$ is measured from the normal to the plane. $I_\sigma(E,\theta)$ is the $\sigma$ band intensity as function of the energy $E$ and the angle $\theta$ while $I_\sigma(E)$ is the corresponding transition density, the factor $\frac{1}{2}$ being introduced because there are 2 $\sigma$ electrons. The $\pi$ electrons, on the other hand, give rise to an emission pattern corresponding to dipoles oscillating in the $z$ direction:

$$I_\pi(E,\theta)=I_\pi(E)\sin^2\theta\ .$$

$I_\pi(E,\theta)$ and $I_\pi(E)$ are defined as above for the $\pi$ band. The total emission at any angle is then

$$I(E,\theta)=I_{\sigma}(E)\left[\frac{1+\cos^{2}\theta}{2}\right]+I_{\pi}(E)\sin^{2}\theta\ . \tag{4}$$

Letting $x=\cos^{2}\theta$, we have

$$I(E,x)=\left[\frac{I_{\sigma}(E)}{2}-I_{\pi}(E)\right]x+\left[\frac{I_{\sigma}(E)}{2}+I_{\pi}(E)\right]\ . \tag{5}$$

If we now make a series of emission band measurements at different angles, and normalize the bands to the same area, then it is clear that a linear least-squares fit of the intensities measured at different angles at each point in energy with the above equation will allow us to separate the $\sigma$ and $\pi$ transition densities.

## RESULTS AND DISCUSSION

Figure 1 shows our measurement of the soft x-ray emission spectrum of our sample in the energy range 240—420 eV plotted on a logarithmic scale. The dominant feature in the spectrum with peak near 275 eV is the main $K$ emission band of graphite. We have identified the peaks near 350 and 390 eV as being Fe and N impurity emission bands, respectively. (Such impurity emission was even more obtrusive in the HOPG samples we had available.) We shall now argue that the peak near 330 eV is the double $1S$ core hole satellite of graphite.

A simple atomic argument for estimating the energy of the C double core hole satellite places it halfway between the energies of the $1S$ states of C and N.[13] This corresponds approximately to using a screening factor for the $1S$ shell of $\frac{1}{2}$ which agrees with common practice.[14] This estimate places the peak at 343 eV, somewhat higher than the observed value. Hayasi,[15] using a slightly different atomic model, estimated that energy to be 327 eV which compared favorably with a feature he observed in the emission spectrum of $B_4C$.[5] He concluded and we agree that this is the origin of the feature in the spectrum. The fact that it is seen in two different carbon compounds further lends credence to its identification. Furthermore, the relative strength of the satellite to the main band is about 0.1%, which is in good agreement with existing satellite data on other materials.[15,16] Aita *et al.*[17] observed a feature in the x-ray emission spectrum of graphite at 316 eV which they attributed to the double $1S$ core hole satellite. Our measurements and analysis as above lead us to disagree with that assignment.

By rotating the sample holder the satellite was measured for take-off angles between 0° and 80° in increments of 20°. Each of these spectra was corrected for background effects in the following way: First a separate measurement of the Fe $L_{2,3}$ emission band in second order from an iron sample was measured. This was then shifted and broadened slightly and subtracted from the present spectra to yield smooth curves in the energy range above the satellite. Second, a third-order polynomial was fit to this background and subtracted from the spectra. The resulting satellite intensities were divided by $E^3$ to yield a density of states (in the one-electron approximation). The results, normalized to the same area, are shown in Fig. 2.

In all measurements just above a core threshold where the absorption coefficient of the sample may be large, and varying with energy, the possibility of distortion of the measured spectrum by self-absorption must be considered. We studied this effect in two ways. First, we measured the satellite using a beam voltage of 1500 V, subtracted the background, and compared with the 3000-V results. The difference in satellite intensity relative to the main band for the two beam voltages indicated a self-absorption reduction at 3 KV of about 50%. The energy dependence of the absorption coefficient of graphite in this energy

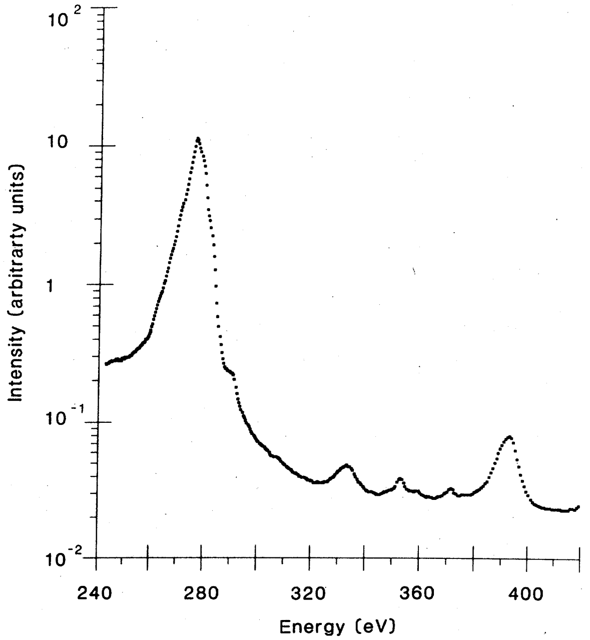

FIG. 1. Soft x-ray emission spectrum of graphite between 240 and 420 eV. Take-off angle is 0° from the c axis and the electron beam energy is 3.0 keV.

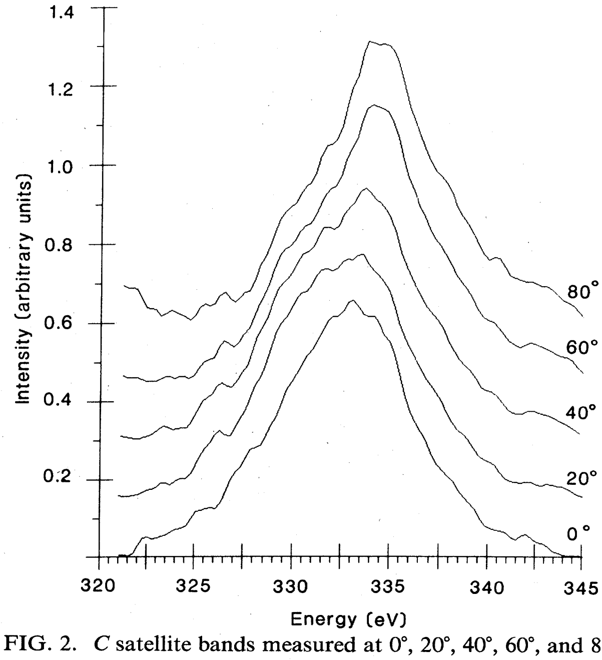

FIG. 2. $C$ satellite bands measured at 0°, 20°, 40°, 60°, and 80° take-off angle, and normalized to the same area.

range has been determined.[18] Over the range 327–337 eV, the full width at half maximum of the satellite, the absorption coefficient is slowly varying and distorts the shapes of these measured satellite curves by less than 5%. This is less than the noise level and can be ignored.

Using angle-dependent data obtained for the main band on this granular sample, and applying Eq. (5) above, we found poor agreement with the shapes of the $\sigma$ and $\pi$ bands obtained in our laboratory from HOPG. Inspection of the sample by microscope indicated that it consisted mainly of grains lying flat ($c$ axis perpendicular to the substrate) with some rotated 90° with respect to this orientation. We modified Eq. (5) allowing a fraction of the grains to be so rotated. We found that by choosing the fraction appropriately, we could reproduce the main band $\sigma$ and $\pi$ shapes quite accurately. For this sample the best fit occurred for 80% lying flat, 20% rotated. This same procedure, with these percentages was used then to analyze the data of Fig. 2. The resulting separation into $\sigma$ and $\pi$ bands is shown in Fig. 3. Figure 4 shows the satellite bands shifted by 56.8 eV, normalized to the area of their corresponding parents, and superimposed on the main $\sigma$ and $\pi$ bands of graphite.

The satellite $\sigma$ band extends from 322 eV up to 342 eV approximately with a maximum at about 332 eV and appears quite similar in shape to that of the main band, although it is somewhat wider and has a little more strength at low energies. The shape of the $\pi$ band on the other hand is significantly distorted. It extends from about 331 to 346 eV and exhibits two different structural features: a maximum at about 335 eV and a weaker shoulder at about 340 eV. The high-energy edges agree fairly well, although the satellite data are rather noisy here, but what is a shoulder in the main band has become a major peak in the satellite on the low-energy side. Strength from the top part of the $\pi$ band has been pulled down towards the bottom of the band. These results are similar to those obtained for simple metals by Mahan[19] and von Berth and Grossmann.[20] The extra core hole is attempting to form an exciton. It enhances the low-energy part of the band in the same way the core hole does in an absorption event. This is a striking example of the final-state rule.[19,20]

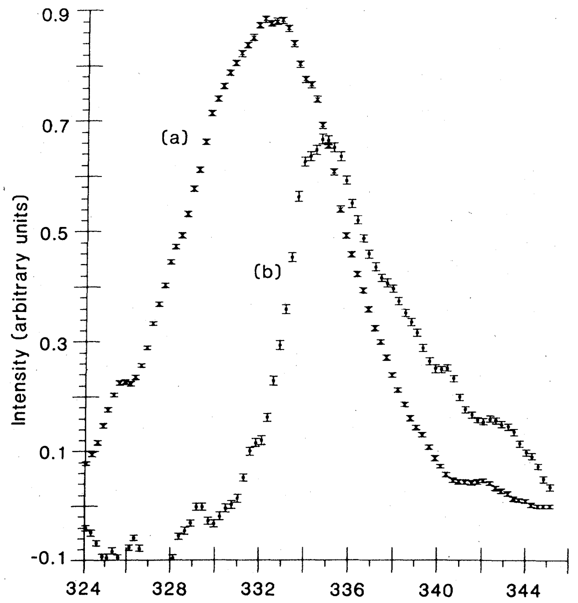

FIG. 3. (a) $\sigma$ band and (b) $\pi$ band of the double core hole satellite. Error bars indicate the statistical uncertainty for each data point.

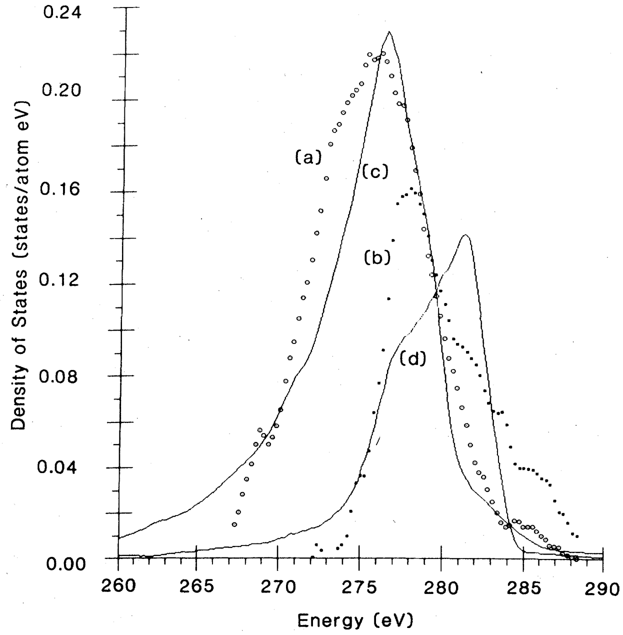

FIG. 4. Satellite and parent $\sigma$ and $\pi$ sub-bands of graphite. Satellite bands are shifted in energy by 56.8 eV and normalized to the area of their corresponding parents. Intensity is expressed in density-of-states units. (a) satellite $\sigma$ band, (b) satellite $\pi$ band, (c) main $\sigma$ band, (d) main $\pi$ band.

We have no immediate explanation of why the $\pi$ band is distorted more than the $\sigma$ band. This is unexpected since the $\sigma$ band consists of $2S$ and $2P$ states, while the $\pi$ band only contains $2P$ electrons. We would have thought that the $2S$ state would have been more strongly affected by the core hole than the $2P$. We are not aware of any theoretical calculation of these spectra for comparison.

Another new feature observed in these spectra is visible in Fig. 1 as a small shoulder near 291 eV. This shoulder is consistently present in all our spectra, and we have been unable to identify any impurity emission to which it could correspond. Applying the modified Eq. (5) to this energy range, we find that this shoulder is entirely of $\sigma$ character. Figure 5 shows an expanded plot of the $\sigma$ and $\pi$ components of the spectrum in this region.

We have often observed in the emission spectra of insulators that emission is visible from electrons excited to the bottom of the conduction band. In certain materials electrons are excited to the conduction band by the incident beam at a sufficiently high rate, and live long enough at the bottom of the conduction band, that they contribute noticeably to the emission spectrum. Here we see a feature 7 eV above the Fermi energy of 284.0 eV,[21] having $\sigma$ character.

According to the calculations of Zunger[22] and Painter and Ellis,[23] the bottom of the conduction band lies 8.0 and 7.5 eV above the Fermi energy. According to the photo-

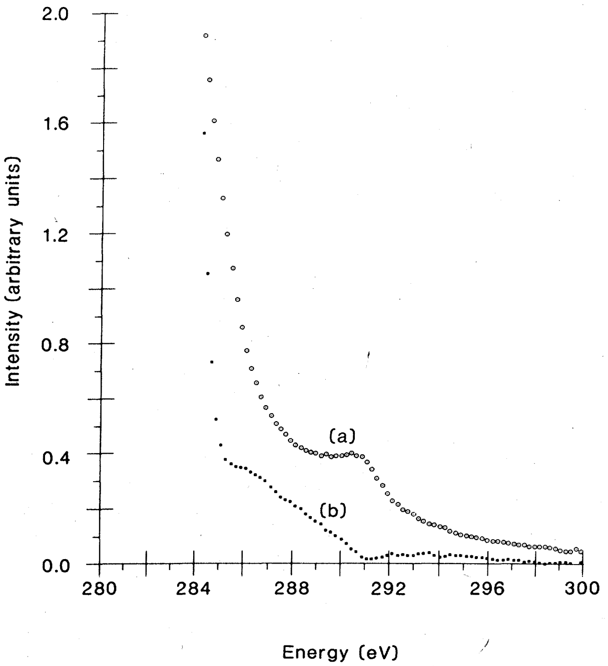

FIG. 5. $\sigma$ and $\pi$ components of the C $K$-emission spectrum between 280 and 300 eV. (a) $\sigma$ intensity, (b) $\pi$ intensity.

emission and secondary-electron-emission measurements of Willis *et al.*[24,25] it lies 7.7 eV above $E_F$. Our result is close to but somewhat smaller than these determinations. This discrepancy could be due to an excitonic binding energy of $0.7\pm0.3$ eV.

It is striking that this feature is observable at all since this $\sigma$ state is degenerate with a continuum of $\pi$ states leading all the way down to the Fermi energy. Two things, however, retard the decay of the $\sigma$ state into a $\pi$ state. First, the $\sigma$ state must rotate 90° to become a $\pi$ state. The torque available to produce this rotation is caused by the spin-orbit interaction, which however is small (a few meV).[26] Second, even if it could rotate, the $\sigma$ band minimum does not lie at the same point in the Brillouin zone as the $\pi$ states with which it is degenerate. Therefore both angular momentum conservation and linear momentum conservation serve to make such a transition doubly forbidden, and allow this feature to appear in our spectra.

## ACKNOWLEDGMENTS

We wish to thank the other members of the laboratory, A. Cafolla, D. Husk, P. Livins, and J. Nithianandam, for helpful suggestions and discussions throughout the course of this work. This work was supported in part by National Science Foundation Grant No. DMR-8214968.

---

[1] M. Siegbahn and W. Stenstrum, Z. Phys. **17**, 48 (1916); **17**, 318 (1916).

[2] F. R. Hirsh, Rev. Mod. Phys. **14**, 45 (1942).

[3] G. B. Doedhar, Natl. Acad. Sci. India A **32**, 320 (1962).

[4] S. J. Edwards, Contemp. Phys. **11**, 195 (1970).

[5] Y. Hayasi, Sci. Rep. Tohoku Univ. **51**, 43 (1968).

[6] W. Burghard, M. Umeno, G. Wiech, and W. Zahorowski, J. Phys. C **16**, 4243 (1983).

[7] T. Sagawa, J. Phys. Soc. Jpn. **21**, 49 (1966).

[8] U. Berg, G. Dräger, and O. Brümmer, Phys. Status Solidi B **74**, 341 (1976).

[9] J. Keiser, Z. Phys. B **26**, 1 (1977).

[10] G. Wiech and W. Zahorowski, in *Inner-Shell and X-ray Physics of Atoms and Solids,* edited by D. J. Fabian, H. Kleinpoppen, and L. M. Watson (Plenum, New York, 1980), p. 815, and references therein.

[11] T. Aton, C. Franck, E. Källne, S. Schnatterly, and F. Zutavern, Nucl. Instrum. Methods **172**, 173 (1980); **172**, 351 (1980).

[12] R. D. Carson, C. P. Franck, S. Schnatterly, and F. Zutavern, Rev. Sci. Instrum. **55**, 1973 (1984).

[13] L. H. Jenkins and D. M. Zehner, Solid State Commun. **12**, 1149 (1973).

[14] H. P. Kelly (private communication).

[15] Y. Hayasi, Sci. Rep. Tohoku Univ. **52**, 41 (1969).

[16] W. F. Hanson and E. T. Arakawa, Z. Phys. **251**, 271 (1972).

[17] O. Aito *et al.*, J. Phys. Soc. Jpn. **30**, 516 (1971).

[18] R. D. Leapman, P. L. Fejes, and J. Silcox, Phys. Rev. B **28**, 2361 (1983).

[19] G. D. Mahan, Phys. Rev. B **21**, 1421 (1980).

[20] U. von Barth and G. Grossmann, Phys. Rev. B **25**, 5150 (1982).

[21] C. P. Franck *et al.*, Phys. Rev. B **31**, 5366 (1985).

[22] A. Zunger, Phys. Rev. B **17**, 626 (1976).

[23] G. S. Painter and D. E. Ellis, Phys. Rev. B **1**, 4747 (1970).

[24] R. F. Willis, B. Feuerbacher, and B. Fitton, Phys. Rev. B **4**, 2441 (1971).

[25] R. F. Willis, B. Fitton, and G. S. Painter, Phys. Rev. B **9**, 1926 (1974).

[26] C. E. Moore, *Atomic Energy Levels,* Natl. Bur. Stand. (U.S.), Natl. Stand. Ref. Data Ser. No. 35 (U.S. GPO, Washington, D.C., 1949), Vol. 1.